Supplementary Material

N-doped sponge-like biochar: A promising CO_2 sorbent for CO_2/CH_4 and CO_2/N_2 gas separation

Mirtha A. O. Lourenço[1,2], Tânia Frade[3], Marta Bordonhos[2,3], Micaela Castellino[4], Moisés L. Pinto[3], Sergio Bocchini[1,4]*

[1] Istituto Italiano di Tecnologia - IIT, Centre for Sustainable Future Technologies (CSFT), Via Livorno 60, 10144-Torino, Italy

[2] CICECO - Instituto de Materiais de Aveiro, Departamento de Química, Universidade de Aveiro, Campus Universitário de Santiago, 3810-193, Aveiro, Portugal

[3] CERENA, Departamento de Engenharia Química, Instituto Superior Técnico, Universidade de Lisboa, 1049-001, Lisboa, Portugal

[4] Department of Applied Science and Technology (DISAT), Politecnico di Torino, Corso Duca degli Abruzzi 24, 10129-Torino, Italy

*Corresponding author: mirtha@ua.pt

Materials characterization

The thermogravimetric analysis coupled with Fourier transform infrared spectroscopy (TGA-IR) was carried out on about 3 mg of each sample using a TG 209 F1 Libra® (NETZSCH GmbH), at 5 °C/min heating rate, from 25 °C to 400, 600 or 800 °C under N_2 flow (40 cm^3/min), depending on the pyrolysis process to mimic. A step at 200 °C for 120 min is performed for the preparation of all samples. Experimental error was estimated to be typically less than 0.05 mg (approximately ± 2.5%). Gas transmittance spectra of the evolved gases were collected on a Bruker Tensor II equipped with IR gas cell (TGA–IR) heated at 200 °C to avoid condensation of degraded products. The instruments were coupled by Netzsch FT-IR Coupling Systems transfer line heated at 230 °C. In order to have a stable infrared (IR) background, the line was cleaned using vacuum during 3 cycles of vacuum/refill with N_2. IR spectra of the evolved gases were sampled at 3 °C (ca. 10 s) intervals. The FTIR analysis was collected in the absorbance mode in the range 650 – 4400 cm^{-1}. The different gases were compared with reference spectra from data bases: ammonia (NH_3) [1], water (H_2O) [2], carbon monoxide (CO) [3], carbon dioxide (CO_2) [4], and acetic acid [5].

Elemental analyses CHN was performed with a Fisons Instruments EA-1108 CHNS-O Element Analyzer. The complete oxidation of the sample was achieved at 1000 ºC. The resulting combustion gases were carried with helium (99.99%) to the chromatographic column where they were separated and quantitatively detected.

X-ray photoelectron spectroscopy (XPS) was performed with a PHI 5000 Versaprobe spectrometer (Physical Electronics, Chanhassen, US), equipped with monochromatic Al K-alpha X-ray source (1486.6 eV). A charge compensation system, based on an electron gun and Ar+ ion gun, was used to neutralize surface charging. Survey and high resolution (HR) spectra are acquired using pass energy (PE) values of 187.85 and 23.50 eV, respectively. The

calibration of the binding energy (BE) scale was achieved by fixing the C–C sp^2 component of the C1s region of the photoelectron spectrum to 284.5 eV. Casa XPS Version 2.3.18 dedicated software was used to analyze the spectra. The Shirley background function [6] was subtracted from HR spectra to remove the background signal.

TGA was performed on a Thermogravimetric Analyzer (TGA) NETZSCH TG209 F1Libra instrument. Approximately 3 mg of sample in alumina pans are heated from 30 to 1000 °C under N_2 flux (20 mL/min), nitrogen flow is used as protection gas (20 mL/min).

77 K (–196 °C) Nitrogen adsorption/desorption isotherms were acquired using an Autosorb iQ equipment (Quantachrome Instruments, USA). The samples are degassed at 120 °C for 8 h.

The biochar morphology was observed by using Field Emission Scanning Electron Microscopy (FESEM) with a Zeiss Supra 40 microscope (Zeiss, Oberkochen, Germany).

Gas adsorption experiments

Volumetric apparatus

The adsorption isotherms of carbon dioxide (CO_2; Air Liquide ALPHAGAZ, 99.998 %), methane (CH_4; Air Liquide ALPHAGAZ, 99.995 %), and nitrogen (N_2; Air Liquide ALPHAGAZ, 99.999 %) were measured on the chitosan-based materials, at 0 ºC (only for CO_2), 25 and 35 ºC and pressures up to 1000 kPa, using the volumetric method. The samples were degassed at 120 °C for 30 min, at heating rate of 5 °C/min, under vacuum of 10^{-6} hPa, after a pre-activation of 12 h, at the same conditions. The gas adsorption was measured on a lab-made stainless steel volumetric apparatus, equipped with a pressure transducer. A stirred thermostatic bath was used to control the temperature of the sample and the adsorption system.

Each experimental pure component adsorption isotherm was fitted using the Virial model and the non-ideality of the gas phase was considered using the second and third virial coefficients. Mean selectivity values were estimated using a method proposed by Myers [7] and the implementation was described in previous works [8,9]. The heats of adsorption for CO_2 were calculated via the Clausius–Clapeyron approach with the viral coefficients estimated from the isotherms at 25 and 35 °C [10].

ynamic Vapor Sorption

Pure CO_2 adsorption isotherm was performed using a Surface Measurement System, Dynamic Vapor Sorption (DVS) Instrument. The best performing materials was selected and previously activated under vacuum of 10^{-4} hPa at 120 ºC for 30 min before starting each measurement. The CO_2 gas was used as provided by Rivoira (Italy), with a purity of 99.99%. The isotherm temperature was kept at 30 °C with increasing pressure (P/P_0 = 5% each step) up to 89 kPa in semi-static conditions (max flowrate = 50 mL·min^{-1}); each step was kept up to equilibrium (criterion dm/dt = 0.001 %·min^{-1}). The desorption measurement was performed by reducing the pressure (P/P_0 = 5% each step) applying the criterion dm/dt = 0.001 %·min^{-1} to reach the equilibrium.

Pure CO_2 adsorption isobar was also performed using the same instrument. The pressure was kept at 89 kPa in semi-static conditions (maximum flowrate = 50 mL·min^{-1}) with an increasing temperature of 10 °C for each step until 80 °C; each isotherm was kept up to equilibrium (criterion dm/dt = 0.01 %·min^{-1}). The reversing procedure was made by decreasing the temperature in 10 °C for each step until 30 °C, and an equilibrium criterion dm/dt of 0.01 %·min^{-1}.

The reusability of the most promising sample was tested by 10 consecutive CO_2 adsorption-desorption cycles. Each cycle combines a CO_2 adsorption measurement at 20 kPa and 30 °C

(with a flowrate = 50 mL·min^{-1} and an equilibrium criterion = 0.02 %·min^{-1}) and a desorption measurement at 80 °C under vacuum of 10^{-4} hPa (criterion dm/dt = 0.02 %·min^{-1}).

The water vapor adsorption isotherm was performed at 30 ºC using the same equipment. The water vapor is taken from the vapor in equilibrium in a flask filled with ultrapure water (Milli-Q). The pressure was increased up to ~4 kPa, by introducing a water vapor pressure of ~1.06 kPa each step (with a max target vapor flow = 15 sccm and an equilibrium criterion dm/dt = 0.001 %·min^{-1}). The desorption measurement was made by decreasing the pressure (1.06 kPa each step) and applying an equilibrium criterion dm/dt = 0.001 %·min^{-1}.

The CTO_P600 sample was also tested in the H_2O/CO_2 adsorption isotherms at 30 °C under continuous gas flow. In this case, the water vapor generated was combined with a separate stream of pure CO_2 before being introduced into the balance. The partial pressure of the gases was controlled by altering the flow rates of these two streams and hence the ratio of the total pressure. Three cycles were conducted to examine various H_2O/CO_2 ratios (maximum total pressure = ~3.8 kPa, 1^{s}t cycle = ~1.06 kPa and ~2.76 kPa, 2nd cycle = ~2.12 kPa and ~1.70 kPa, and 3rd cycle = ~3.18 kPa and ~0.64 kPa of H_2O and CO_2, respectively), and the equilibrium criterion used was dm/dt = 0.001%·min^{-1}. The desorption procedure was performed under the reverse conditions of the adsorption measurement.

TGA

The CO_2 adsorption performance over N_2 gas was evaluated using a TGA (NETZSCH TG 209F1 Libra) apparatus using the same procedure previously described in reference [11]. The measurements were performed at 35 °C and environmental pressure (~100 kPa). The samples (~10 mg) were degassed through 3 consecutive cycles of vacuum and pure N_2, followed by heating the samples until 120 °C (heating rate = 40 °C·min^{-1}) under vacuum for 30 min. After cooling to 35 °C (cooling rate = 2 °C·min^{-1}), the biochar samples were exposed to pure N_2

(flowrate = 40 mL·min^{-1}) at atmospheric pressure for 30 min, until weight stabilization. Then, the N_2 gas was swept with a mixture of CO_2/N_2 (20 vol.% of CO_2, total flowrate = 40 mL·min^{-1}) for 120 min. Both CO_2 and N_2 flow rates were kept constant. The weight difference between the initial and final moment of the CO_2 adsorption indicates the CO_2 amount adsorbed by the materials. Finally, the desorption of the CO_2 was studied under pure N_2 (flowrate = 40 mL·min^{-1}) at atmospheric pressure with increasing temperature until 100 °C (heating rate = 40 °C·min^{-1}).

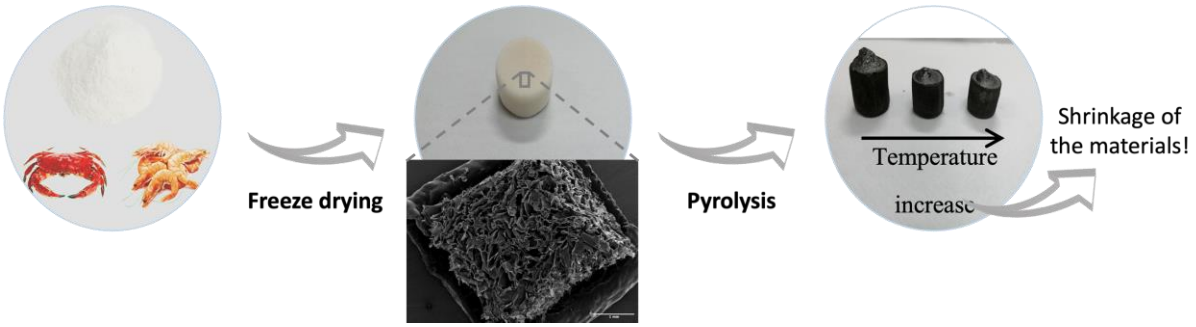

Scheme S1. Schematic representation of the synthesized biochar materials and SEM image of the chitosan aerogel material.

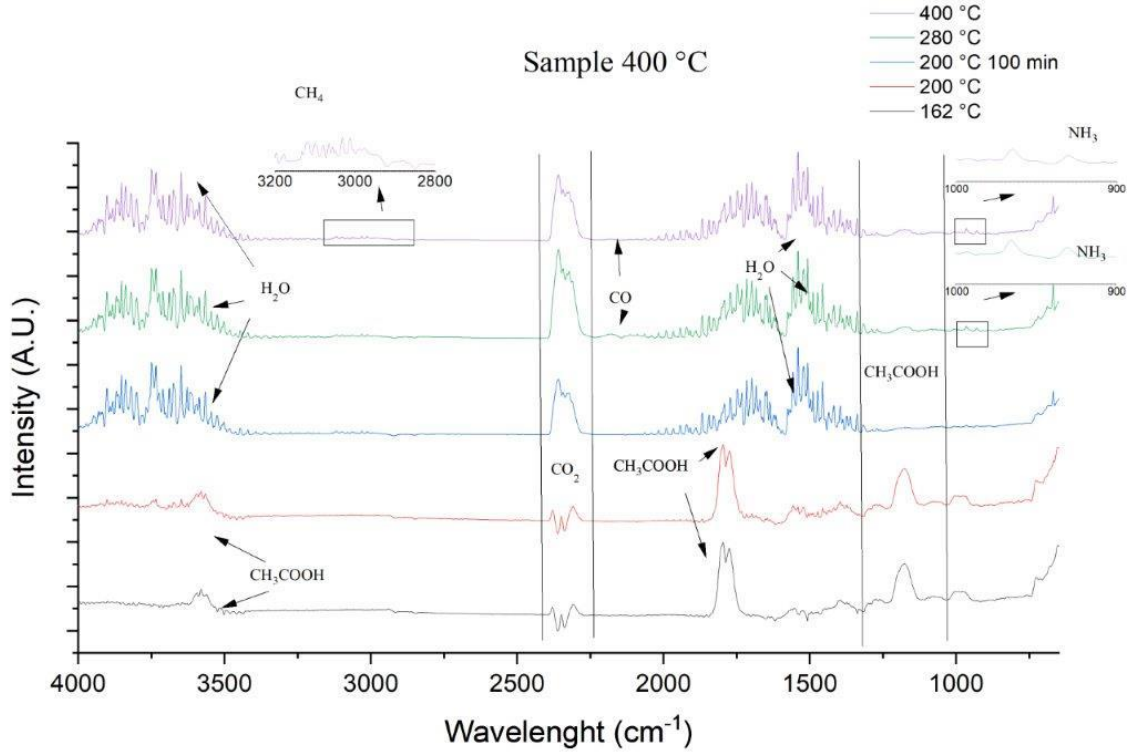

Figure S1. IR spectra of the developed gases at 162, 200, 200 (at 100 min.), 280 and 400 °C under N_2 flow, acquired during the pyrolysis process to obtain CTO_P400 sample.

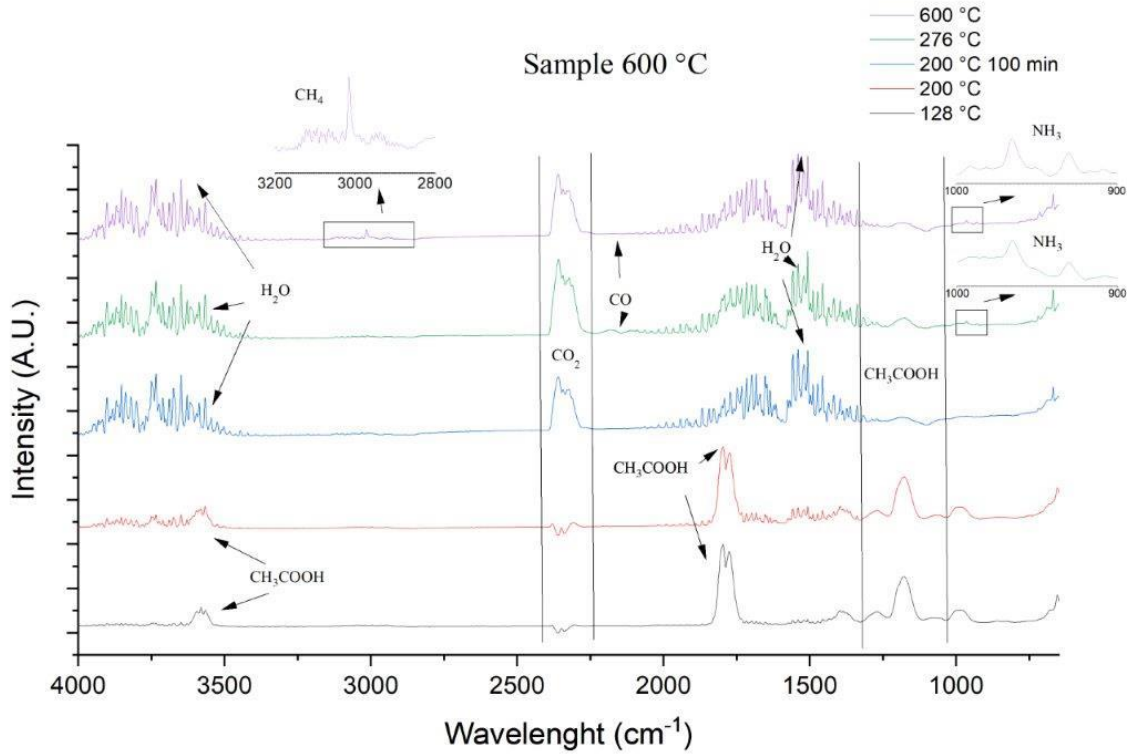

Figure S2. IR spectra of the developed gases at 128, 200, 200 (at 100 min.), 276 and 600 °C under N_2 flow, acquired during the pyrolysis process to obtain CTO_P600 sample.

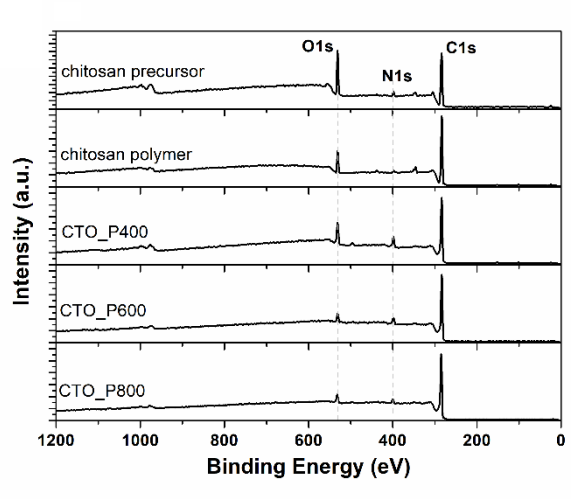

Figure S3. XPS survey spectra for chitosan precursor and polymer samples and pyrolyzed samples (CTO_P400, CTO_P600, CTO_P800) from top to bottom.

Table S1. Elemental analyses of the pyrolyzed chitosan.

Sample	**% N**	**% C**	**% H**
CTO_P400	9.87	64.44	3.59
CTO_P600	8.88	71.55	<2
CTO_P800	6.40	70.20	<2

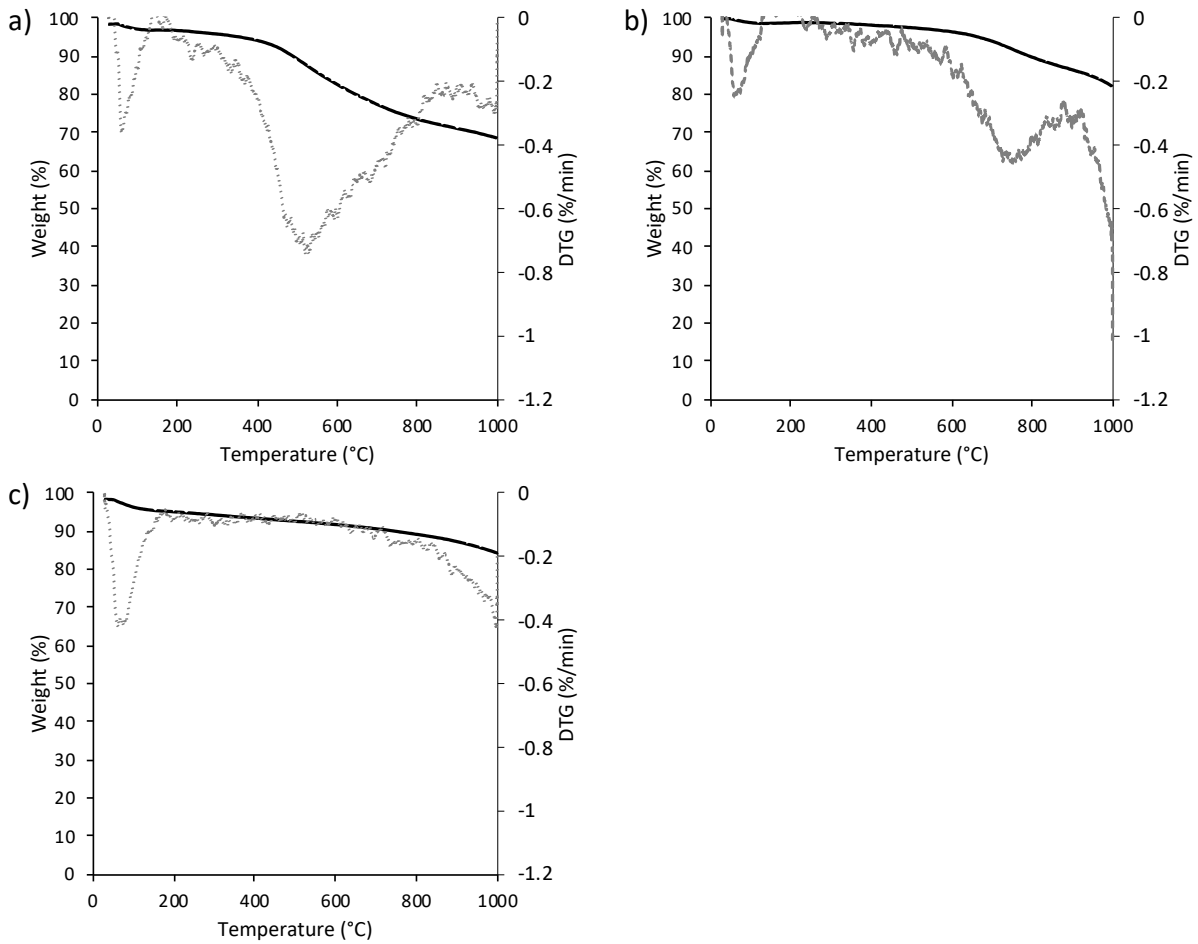

Figure S4. TGA of a) CTO_P400, b) CTO_P600, and c) CTO_P800 under N_2 atmosphere.

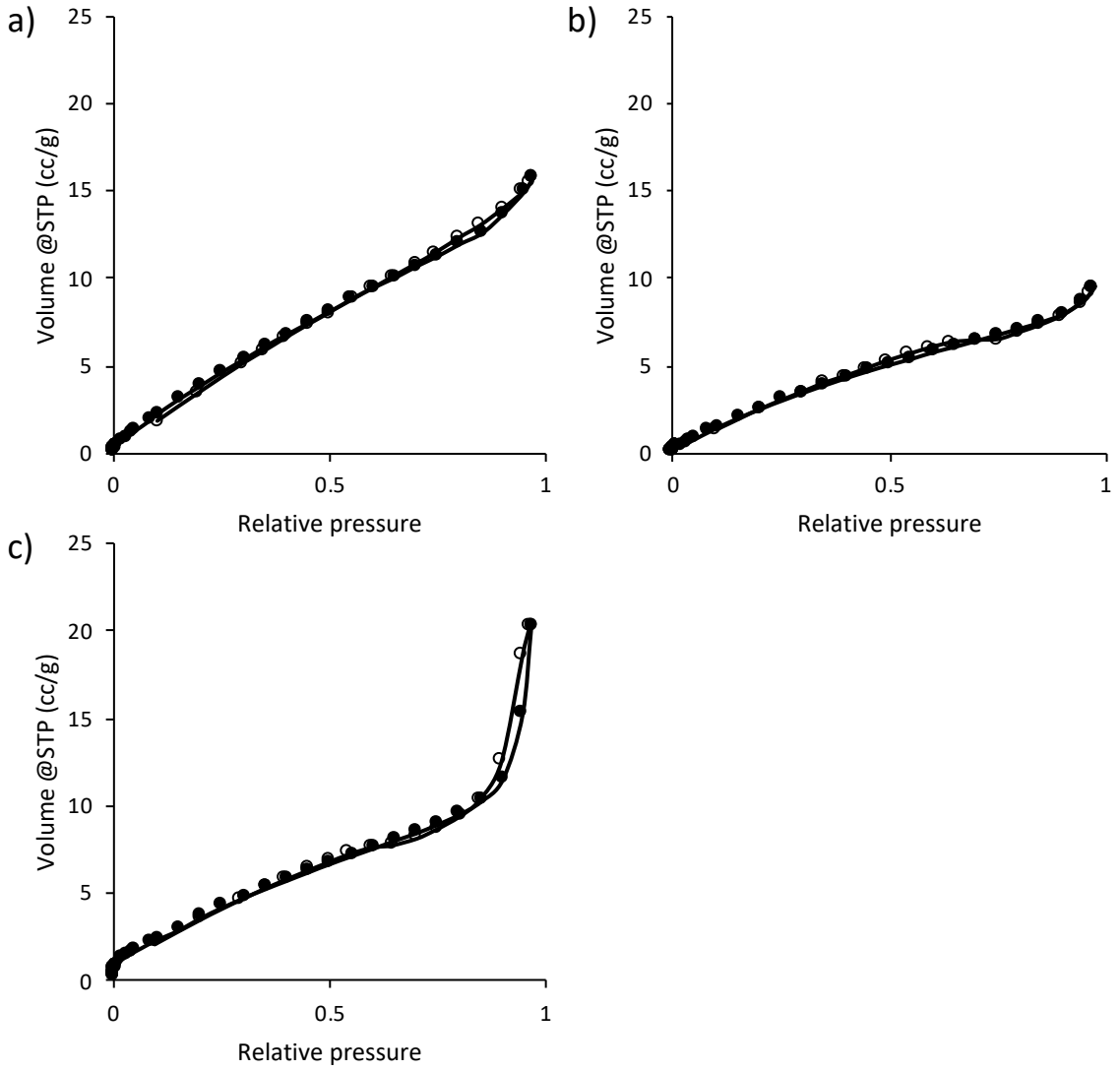

Figure S5. 77 K (−196 °C) N_2 adsorption-desorption isotherms of a) CTO_P400, b) CTO_P600, and c) CTO_P800 (filled symbols correspond to adsorption process, empty symbols correspond to desorption process).

Table S2. Textural parameter determined by 77 K **(**−196 °C) N_2 adsorption-desorption isotherms and 0 °C CO_2 adsorption isotherms of CTO_P*x*.

Sample	S_{BET} ($m^2 \cdot g^{-1}$)[a]	R^b	V_p ($cm^3 \cdot g^{-1}$)[c]	S_{BET}^{micro} ($m^2 \cdot g^{-1}$)[d]	R^b	*DR*, V_p^{micro} ($cm^3 \cdot g^{-1}$)[e]	*NLDFT*, V_p^{micro} ($cm^3 \cdot g^{-1}$)[e]	*MC*, V_p^{micro} ($cm^3 \cdot g^{-1}$)[e]
CTO_P400	18.54	0.9877	0.023	133	0.9993	0.080±0.0014	0.068±0.0004	0.077±0.0006
CTO_P600	11.55	0.9874	0.013	260	0.9992	0.134±0.0027	0.111±0.0061	0.102±0.0013
CTO_P800	14.58	0.9987	0.030	-	-	-	-	-

[a] Brunauer-Emmett-Teller (BET) Specific surface area determined by using 77 K (−196 °C) N_2 adsorption isotherms; [b] Correlation coefficient; [c] V_p denotes pore volume determined from 77 K (−196 °C) N_2 adsorption isotherms; [d] BET Specific surface area determined by using 0 °C CO_2 adsorption isotherms and applying the nonlocal density functional theory (NLDFT); [e] pore volume determined from 0 °C CO_2 adsorption isotherm and applying Dubinin-Radushkevich (DR), NLDFT and Monte Carlo (MC) models.

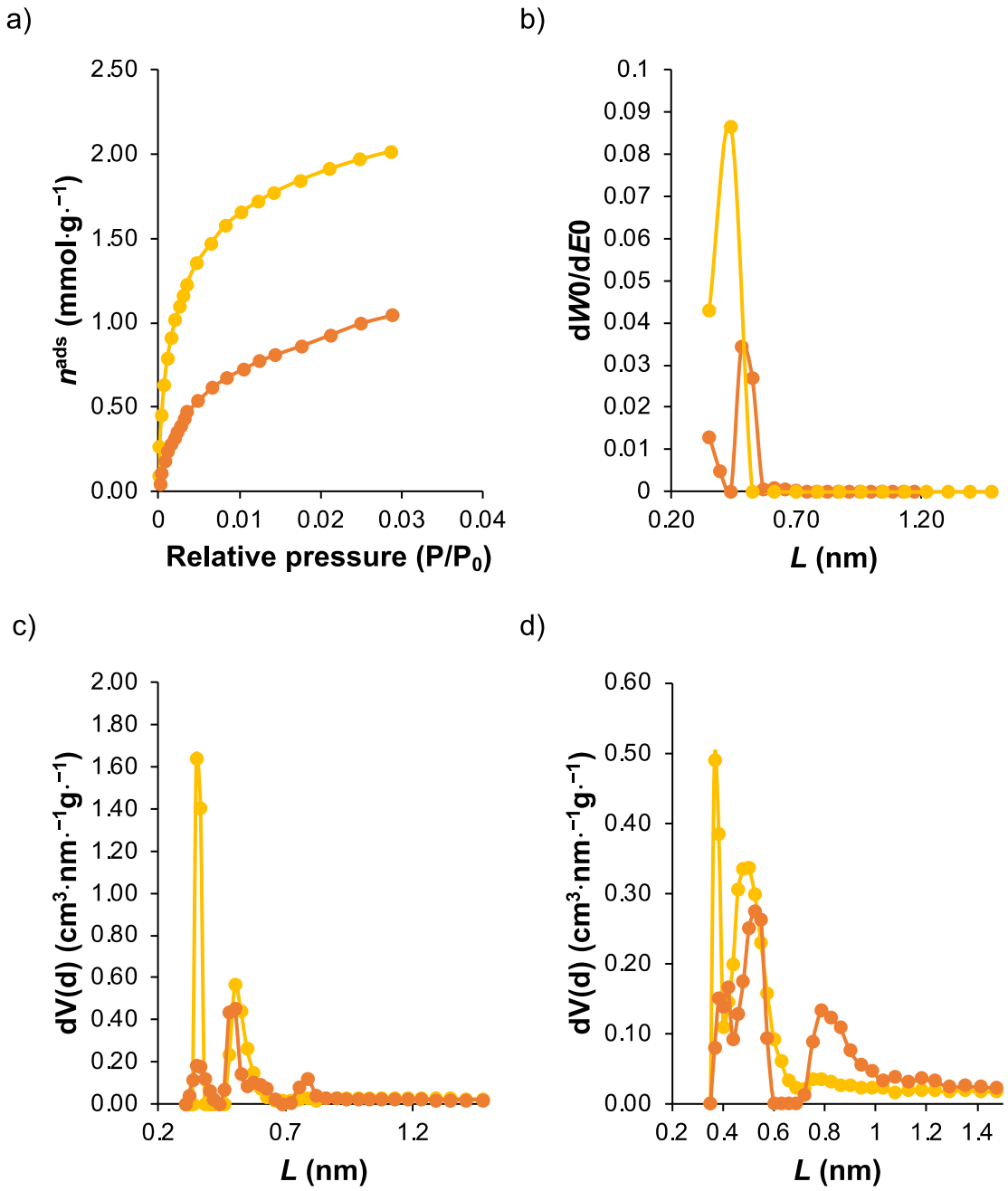

Figure S6. a) CO_2 adsorption isotherm at 0 °C and pore size distribution curves determined using the b) DR, c) NLDFT, and d) MC models on CTO_P400 (orange) and CTO_P600 samples (yellow).

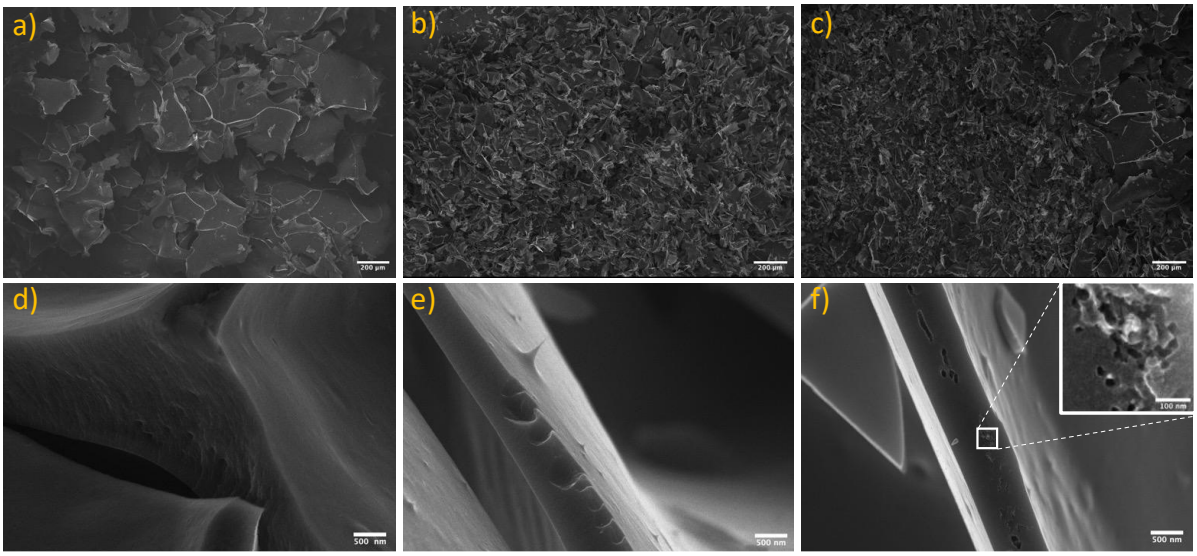

Figure S7. FESEM images of a) CTO_P400, b) CTO_P600, and c) CTO_P800 acquired at a magnification of 500x, and d) CTO_P400, e) CTO_P600, and f) CTO_P800 obtained at a magnification of 50000x.

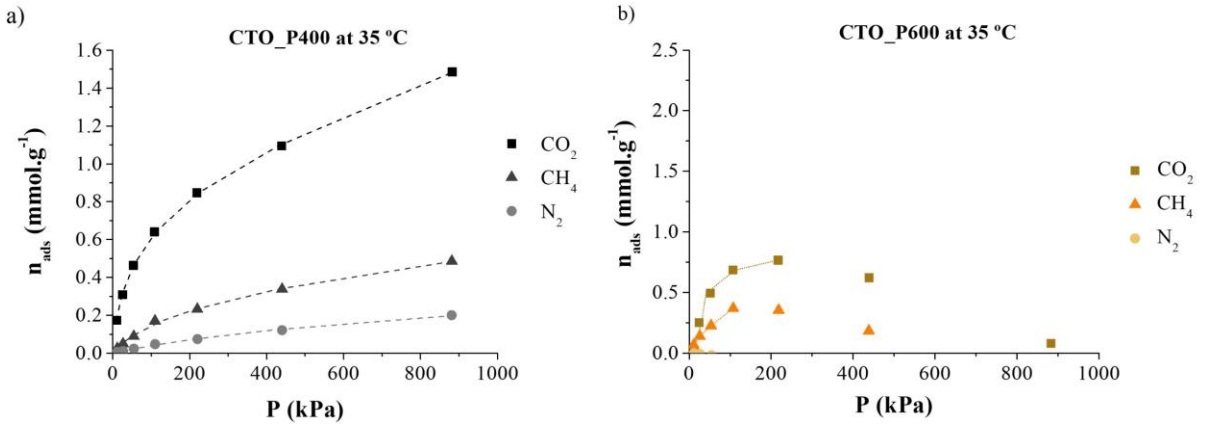

Figure S8. Adsorption isotherms of pure CO_2 (square symbols), CH_4 (triangle symbols), and N_2 (circle symbols) gases at 35 °C in the pyrolyzed samples at: **a)** 400 °C (CTO_P400) and **b)** 600 °C (CTO_P600). The dashed lines represent the fits of the Virial isotherm model to the experimental data.

Table S3. Virial coefficients (C_1 and C_2) and Henry constants (K) for the adsorption of methane, carbon dioxide and nitrogen at 35 ºC on the studied materials.

Gas	Sample	K (mol.kg^{-1}.kPa^{-1})	C_1 (kg.mol^{-1})	C_2 (kg.mol^{-1})^2	C_3 (kg.mol^{-1})^3 *
CH_4	CTO_P400	2.61×10^{-3}	4.32	-2.28	---
	CTO_P600	7.56×10^{-3}	3.08	-2.52	---
	CTO_P800	---	---	---	---
CO_2	CTO_P400	3.25×10^{-2}	3.25	-0.87	---
	CTO_P600	1.43×10^{-3}	-9.93	11.42	---
	CTO_P800	1.24×10^{-1}	3.38	-0.79	---
N_2	CTO_P400	4.49×10^{-4}	3.48	---	---
	CTO_P600	---	---	---	---
	CTO_P800	---	---	---	---

* The third virial coefficient (C_3) was neglected for all fitted adsorption isotherms.

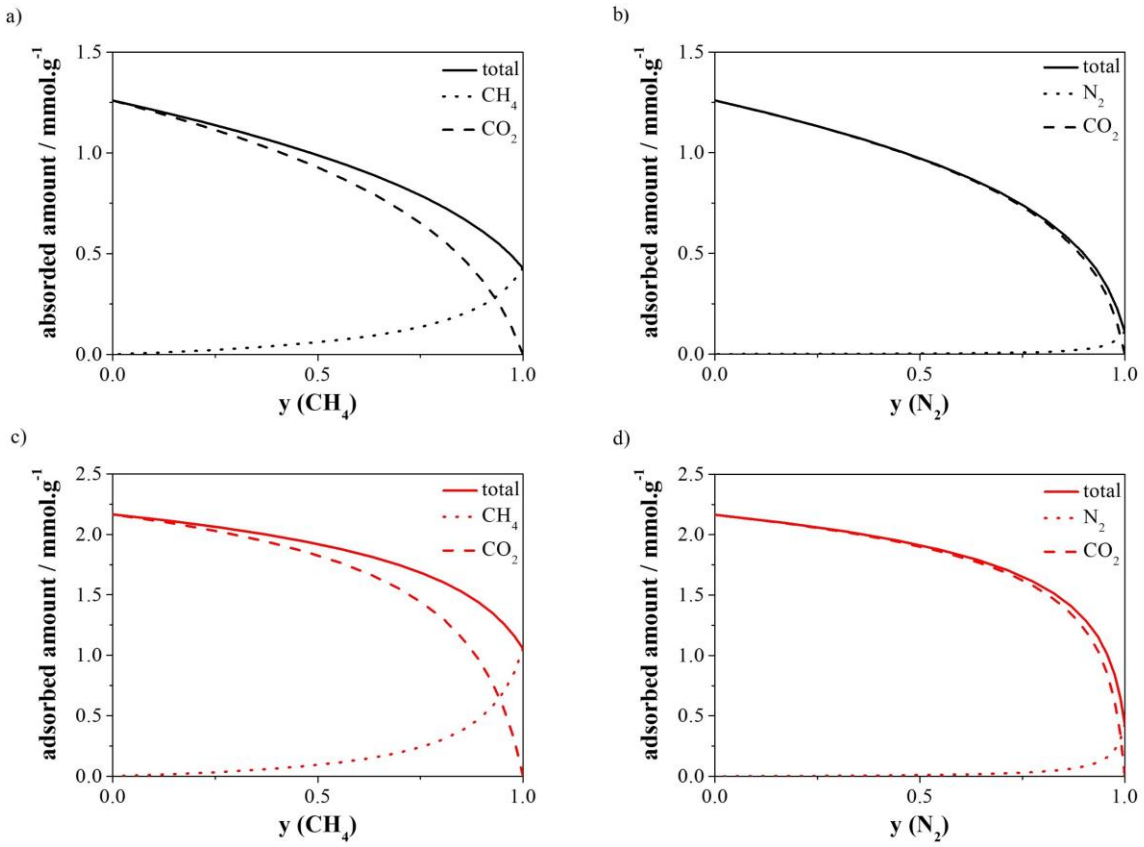

Figure S9. Adsorbed amount of (a) and (c) CH_4/CO_2 and (b) and (d) N_2/CO_2 mixtures as a function of the CH_4 and N_2 molar fraction in the gas phase, respectively, at 500 kPa and 25 °C, for CTO_P400 (black lines) and CTO_P600 (red lines) materials.

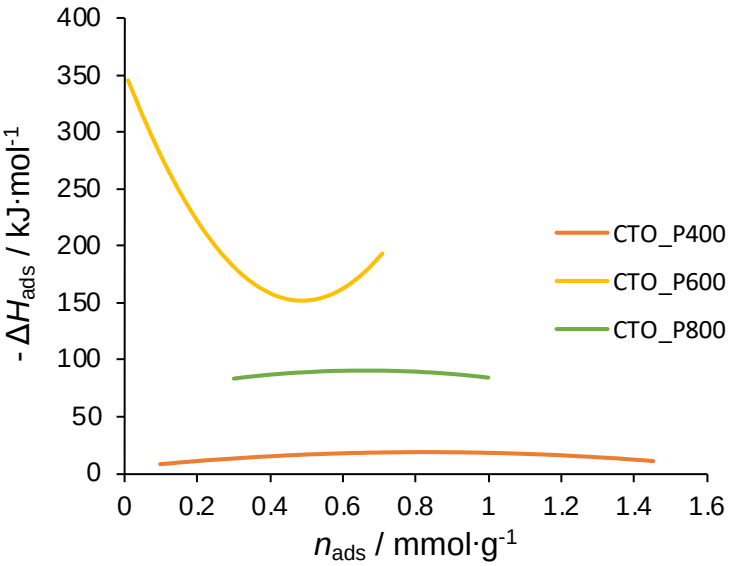

Figure S10. Heats of adsorption for CO_2 calculated via the Clausius–Clapeyron approach with the viral coefficients estimated from the isotherms at 25 and 35 °C.

References:

[1] Ammonia Infrared Spectrum, John Wiley & Sons, Inc. SpectraBase., (n.d.). https://spectrabase.com/spectrum/77SJur7fazW (accessed April 4, 2022).

[2] Water Infrared Spectrum, John Wiley & Sons, Inc. SpectraBase, (n.d.). https://spectrabase.com/spectrum/BnpcCEB1yUv (accessed April 4, 2022).

[3] Carbon Monoxide Infrared Spectrum, John Wiley & Sons, Inc. SpectraBase, (n.d.). https://spectrabase.com/spectrum/Big2BLmUPf2 (accessed April 4, 2022).

[4] Carbon Dioxide Infrared Spectrum, John Wiley & Sons, Inc. SpectraBase, (n.d.). https://spectrabase.com/spectrum/Big2BLmUPf2 (accessed April 4, 2022).

[5] Acetic acid Infrared Spectrum, John Wiley & Sons, Inc. SpectraBase., (n.d.). https://spectrabase.com/spectrum/2ydLrNZDkJr (accessed April 4, 2022).

[6] D.A. Shirley, High-resolution x-ray photoemission spectrum of the valence bands of gold, Phys Rev B. 5 (1972) 4709–4714. https://doi.org/10.1103/PhysRevB.5.4709.

[7] A.L. Myers, Equation of State for Adsorption of Gases and Their Mixtures in Porous Materials, Adsorption. 9 (2003) 9–16. https://doi.org/10.1023/A:1023807128914.

[8] M.L. Pinto, J. Pires, J. Rocha, Porous Materials Prepared from Clays for the Upgrade of Landfill Gas, The Journal of Physical Chemistry C. 112 (2008) 14394–14402. https://doi.org/10.1021/jp803015d.

[9] J. Pires, V.K. Saini, M.L. Pinto, Studies on selective adsorption of biogas components on pillared clays: Approach for biogas improvement, Environ Sci Technol. 42 (2008) 8727–8732. https://doi.org/10.1021/es8014666.

[10] F. Rouquerol, J. Rouquerol, K. Sing, P. Llewellyn, G. Maurin, Adsorption by Powders and Porous Solids: Principles, Methodology and Applications, 2nd ed., Elsevier Ltd, 2014.

[11] M.A.O. Lourenço, M. Fontana, P. Jagdale, C.F. Pirri, S. Bocchini, Improved CO2 adsorption properties through amine functionalization of multi-walled carbon nanotubes, Chemical Engineering Journal. 414 (2021) 128763. https://doi.org/10.1016/j.cej.2021.128763.